Acta Cryst E CRYSTALLOGRAPHIC COMMUNICATIONS

ISSN 2056-9890

Crystal structure and Hirshfeld surface analysis and energy frameworks of 1-(2,4-dimethylphenyl)-4-(4-methoxyphenyl)naphthalene

U. Mohamooda Sumaya,[a] J. KarunaKaran,[b] K. Biruntha,[a] A. K. MohanaKrishnan[b] and G. Usha[c]*

[a]Department of Physics, Bharathi Women's College (A), Chennai-108, Tamilnadu, India, [b]Department of Organic Chemistry, University of Madras, Chennai-25, Tamilnadu, India, and [c]PG and Research Department of Physics, Queen Mary's College (A), Chennai-4, Tamilnadu, India. *Correspondence e-mail: guqmc@yahoo.com

Received 24 May 2018
Accepted 6 June 2018

Edited by H. Stoeckli-Evans, University of Neuchâtel, Switzerland

Keywords: crystal structure; naphthalene; C—H···π interactions; Hirshfeld surface analysis; two-dimensional fingerprint plots; energy frameworks..

CCDC reference: 1841351

Supporting information: this article has supporting information at journals.iucr.org/e

In the title compound, $C_{25}H_{22}O$, the two rings of the naphthalene system are inclined to each other by 3.06 (15)°. The mean plane of the naphthalene ring system makes a dihedral angle of 65.24 (12)° with the dimethylphenyl ring and 55.82 (12)° with the methoxyphenyl ring. The dimethylphenyl ring is inclined to the methoxyphenyl ring by 59.28 (14)°. In the crystal, adjacent molecules are linked *via* C—H···π interactions, forming chains along [100]. Using Hirshfeld surface and two-dimensional fingerprint plots, the presence of short intermolecular interactions in the crystal structure were analysed. The intermolecular interaction energies were also calculated and their distribution over the crystal structure was visualized graphically using energy frameworks.

1. Chemical context

Naphthalene and its derivatives are known for their wide range of applications in the field of pharmaceuticals. They are also used in the manufacturing of colorants, surface-active agents, resins, disinfectants and insecticides. These derivatives play a vital role in the control of microbial infection (Rokade & Sayyed, 2009) and in the chemical defence against biological enemies (Wright *et al.*, 2000). Compounds with a naphthalene moiety have been shown to exhibit significant anti-TB activity (Upadhayaya *et al.*, 2010).

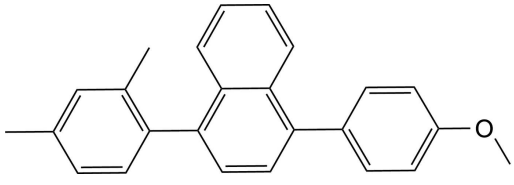

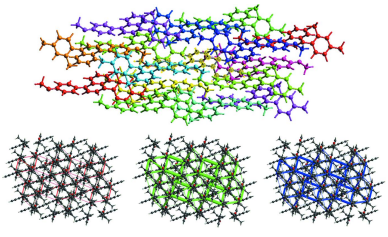

2. Structural commentary

The molecular structure of the title compound is illustrated in Fig. 1. The benzene ring (C9–C14) of the naphthalene moiety is substituted by a dimethylphenyl ring (C2–C4/C6–C8) and a methoxyphenyl ring (C19–C24) *para* to each other. The naphthalene ring system is slightly bent with the two aryl rings being inclined to each other by 3.06 (15)°. Its mean plane makes dihedral angles of 65.24 (12)° with the dimethylphenyl ring (C2–C4/C6–C8) and 55.82 (12)° with methoxyphenyl ring (C19–C24). The latter two rings are inclined to each other by

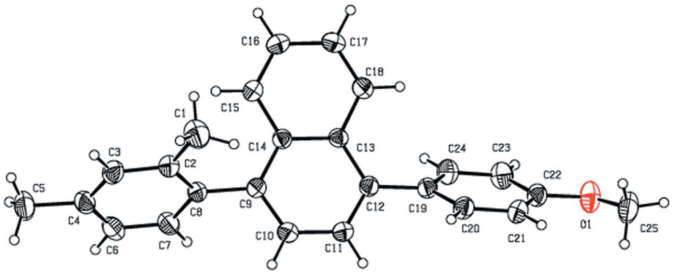

Figure 1
The molecular structure of the title compound, with the atom labelling. Displacement ellipsoids are drawn at 50% probability level.

59.28 (14)°. The methoxy group (C22/O1/C25) lies out of the plane of the benzene ring (C19–C24) to which it is attached by 11.3 (3)°. The bond lengths and bond angles are similar to those reported for 1,4-diphenylnaphthalene, which crystallized with two independent molecules in the asymmetric unit (Lima *et al.*, 2012).

3. Supramolecular features

In the crystal, there is only one significant intermolecular interaction present, *viz*. a C—H···π interaction linking adjacent molecules to form chains propagating along the *a*-axis direction (Table 1 and Fig. 2).

4. Database survey

A search of the Cambridge Structural Database (Version 5.39, last update February 2018; Groom *et al.*, 2016) for the aromatic skeleton of the title compound yielded ten hits. They include 1,4-diphenylnaphthalene itself, which crystallized with two independent molecules in the asymmetric unit (CSD refcode ZAXJEP: Lima *et al.*, 2012). There are also a number of copper(II) complexes (LAYQOU: Chen *et al.*, 2017; BOSHIC: Cai *et al.*, 2014; PUBSOV: Lin *et al.*, 2009) of the tetracarboxylic acid derivative, 5,5′-(naphthalene-1,4-diyl)-diisophthalic acid, all of which are metal–organic frameworks.

5. Analysis of the Hirshfeld surfaces, interaction energies and energy frameworks

The Hirshfeld surfaces and two-dimensional fingerprint plots were generated in order to explore and quantify the weak

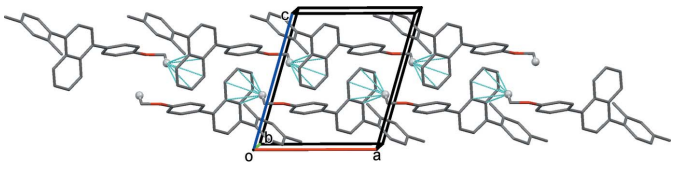

Figure 2
The crystal packing of the title compound, viewed along the *b* axis. The C—H···π interactions (see Table 1) are shown as dashed lines, and only the H atom H25*C* (grey ball) has been included.

Table 1
Hydrogen-bond geometry (Å, °).

Cg is the centroid of the C13–C18 ring.

D—H···*A*	*D*—H	H···*A*	*D*···*A*	*D*—H···*A*
C25—H25*C*···*Cg*^{i}	0.96	2.78	3.597 (5)	144

Symmetry code: (i) $x-1, y, z$.

intermolecular interactions using the program *CrystalExplorer* 17.5 (Turner *et al.*, 2017). The electrostatic potentials were calculated using *TONTO*, integrated in the program *CrystalExplorer* (Spackman *et al.*, 2008; Jayatilaka *et al.*, 2005). The Hirshfeld surfaces of the title compound were mapped over d_{norm}, electrostatic potential, curvedness and shape index (Fig. 3*a*–3*d*); depending upon the closeness to the adjacent molecules, the colour patches are mapped differently on the Hirshfeld surface (Fig. 3*e*). Two-dimensional fingerprint plots showing the result of all intermolecular contacts (McKinnon *et al.*, 2007) are presented in Fig. 4*a*; d_i (*x* axis) and d_e (*y* axis) are the closest internal and external distance from a given point on the Hirshfeld surface. The fingerprint plot of H···H contacts, which represent the largest contribution to the Hirshfeld surface (64.6%), are shown as a distinct pattern with a minimum value of $d_e = d_i \simeq 1.2$ Å (Fig. 4*b*). The C···H/H···C interactions appear as the next largest region of the fingerprint plot, highly concentrated at the edges, having almost the same $d_e + d_i \simeq 2.7$ Å (Fig. 4*c*), with on overall contribution of 27.1%. The O···H/H···O interactions on the fingerprint plot, which contribute 5.2% of the total Hirshfeld surfaces, with $d_e + d_i \simeq 2.8$ Å (Fig. 4*d*) are shown as two symmetrical wings. The C···C contacts, which are the measure of π–π stacking interactions, occupy 3.1% of the Hirshfeld surfaces and appear as a unique triangle at about $d_e = d_i \simeq 1.8$ Å (Fig. 4*e*). These weak interactions mostly contribute to the packing of the title compound.

The interaction energies between the molecules are obtained using monomer wavefunctions at the B3LYP/6-

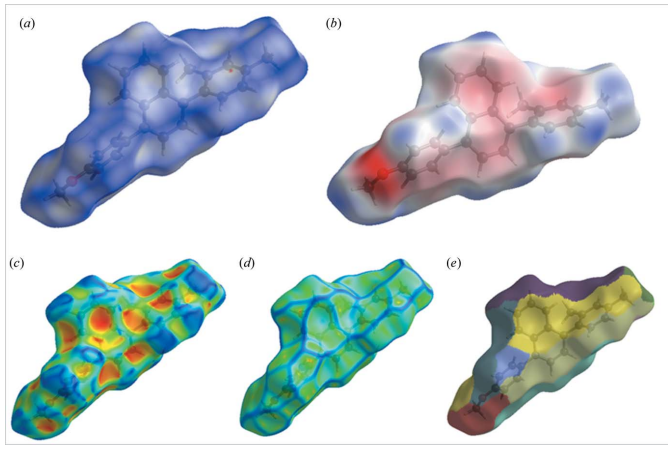

Figure 3
Hirshfeld surfaces mapped over (*a*) d_{norm}, (*b*) electrostatic potential, (*c*) shape index and (*d*) curvedness and (*e*) fragment patches.

Table 2
Scale factors for the benchmarked energy model.

Energy model	k_{elec}	k_{pol}	$k_{energy\text{-}dispersive}$	k_{rep}
CE-B3LYP···B3LYP/6–31G(d,p) electron densities	1.057	0.740	0.871	0.618

31G(p,d) level. The total interaction energy, which is the sum of scaled components, was calculated for a 3.8 Å radius cluster of molecules around the selected molecule (Fig. 5*a*). The scale factors used in the CE-B3LYP benchmarked energy model (Mackenzie *et al.*, 2017) are given in Table 2. The energies calculated by the energy model reveals that the dispersion energy contributes significantly to the interactions in the crystal (Table 3).

The energy framework calculations were performed for a cluster of molecules present in 2 × 2 × 2 unit cells using the CE-B3LYP energy model. Energies between molecular pairs are represented as cylinders joining the centroids of pairs of molecules with the cylinder radius proportional to the magnitude of the interaction energy. Energy frameworks were constructed for E_{elec} as red cylinders, E_{dis} as green and E_{tot} as blue (Fig. 5*b*–5*d*) and these cylinders represent the relative strength of molecular packing in different directions. Thus the supramolecular architecture of the crystal structure is visualized uniquely by energy frameworks.

6. Synthesis and crystallization

A reaction scheme for the synthesis of the title compound is illustrated in Fig. 6. To a solution of *m*-xylyl-*p*-anisyl tethered benzo[*c*]furan (0.16 g, 0.49 mmol) in dry xylenes (15 ml) was added tetrathiafulvalene (TTF) (0.10 g, 0.49 mmol) and the mixture was refluxed until the consumption of benzo[*c*]furan was complete; monitored by the disappearance of the fluorescent colour after 6 h. After the removal of xylenes *in vacuo*,

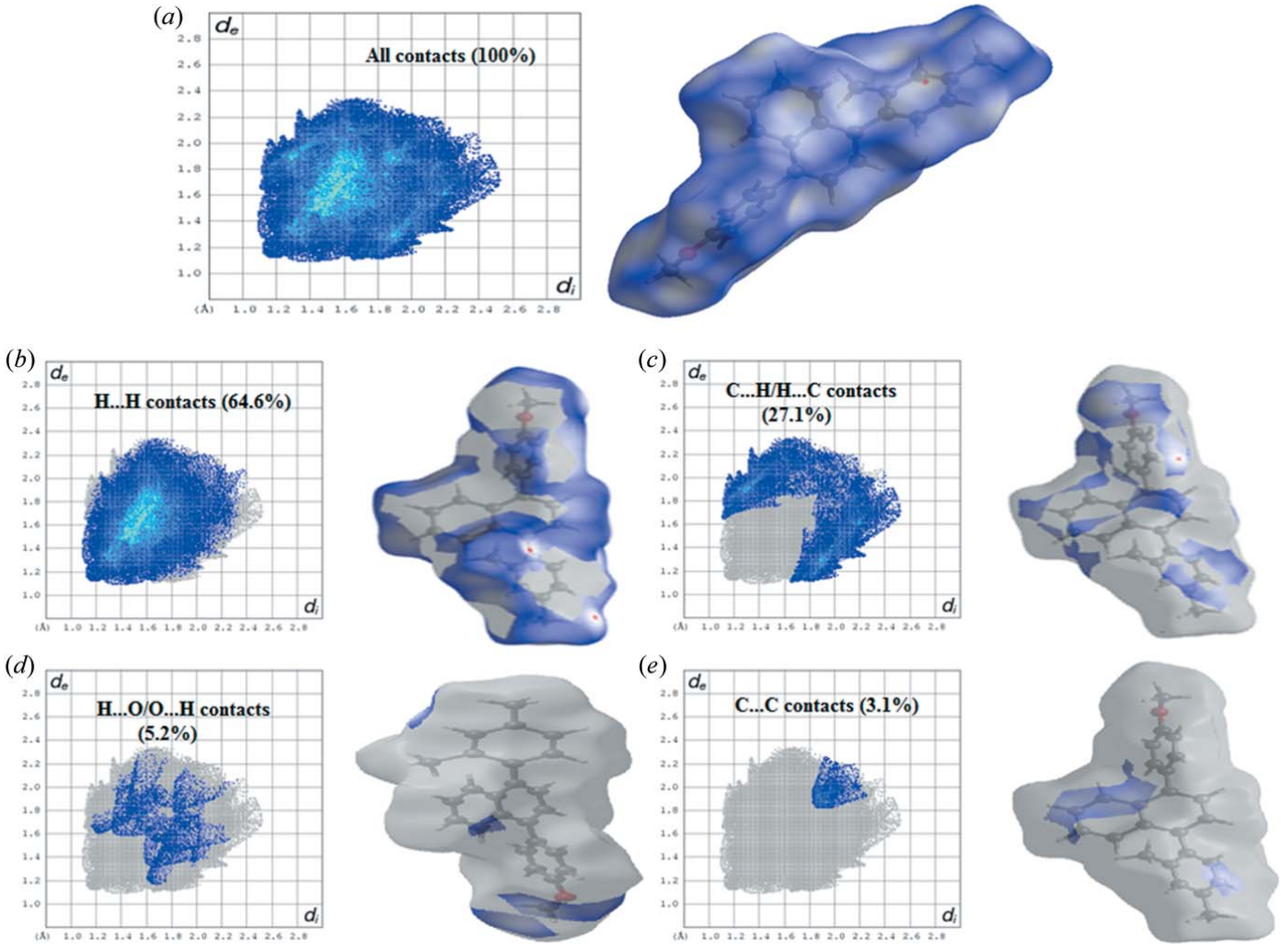

Figure 4
Two-dimensional fingerprint plot for the title compound showing the contributions of individual types of interactions: (*a*) all intermolecular contacts, (*b*) H···H contacts, (*c*) C···H/H···C contacts, (*d*) H···O/O···H contacts, (*e*) C···C contacts. The outline of the full fingerprint is shown in grey. Surfaces to the right highlight the relevant surface patches associated with the specific contacts with d_{norm} mapped.

Table 3
Interaction energies (kJ mol^{-1}).

R is the distance between molecular centroids (mean atomic position) in Å and *N* is the number of molecules at that distance.

Colour	*N*	symop	*R*	E_{elec}	E_{pol}	$E_{energy\text{-}dispersive}$	E_{rep}	E_{total}
Red	2	*x*, *y*, *z*	15.38	−2.2	−0.6	−11.2	6.2	−8.6
Orange	1	−*x*, −*y*, −*z*	15.99	−4.3	−0.8	−11.5	4.2	−12.5
Yellow	1	−*x*, −*y*, −*z*	7.45	−6.2	−1.3	−39.2	19.3	−29.7
Lime	2	*x*, *y*, *z*	9.17	−10.0	−1.8	−44.0	26.8	−33.6
Green	2	*x*, *y*, *z*	10.46	−0.1	−0.1	−6.6	1.5	−5.0
Aquamarine	1	−*x*, −*y*, −*z*	6.86	−6.8	−0.9	−39.9	18.7	−31.0
Cyan	1	−*x*, −*y*, −*z*	10.11	−0.3	−0.4	−19.8	6.7	−13.7
Blue	1	−*x*, −*y*, −*z*	5.37	−3.3	−1.9	−69.2	32.2	−45.2
Violet	1	−*x*, −*y*, −*z*	9.31	−6.5	−0.8	−36.0	20.7	−26.0
Orchid	2	*x*, *y*, *z*	14.01	0.1	0.0	−2.0	0.0	−1.7
Magenta	1	−*x*, −*y*, −*z*	11.61	−3.3	−1.0	−41.6	20.4	−27.9

the crude adduct was dissolved in dry CH_2Cl_2 (15 ml) and then kept at 273 K. To this, triflic acid (0.02 g, 0.13 mmol) was added and the mixture stirred at room temperature for 10 min. After completion of the reaction (monitored by TLC), it was poured into ice–water (20 ml) and then extracted with CH_2Cl_2 (2 × 10 ml). The organic layers were combined and washed with aq. $NaHCO_3$ (2 × 10 ml) and then dried (Na_2SO_4). Removal of the solvent followed by column chromatographic purification (silica gel, 5% ethyl acetate in hexane) afforded the title compound as a yellow solid (0.20 g, 79%). Yellow block-like crystals of the title compound, suitable for X-ray diffraction analysis, were obtained by slow evaporation of a solution in $CHCl_3$ (m.p. 351–353 K).

7. Refinement

Crystal data collection and structure refinement details are summarized in Table 4. All H atoms were positioned geometrically and refined using a riding model: C—H = 0.93–0.96 Å with U_{iso}(H) = 1.5 U_{eq}(C-methyl) and 1.2U_{eq}(C) for other H atoms.

Acknowledgements

The authors thank the Central Instrumentation Facility (DST–FIST), Queen Mary's College (A), Chennai-4, for the computing facilities and the SAIF, IIT, Madras, for the X-ray data collection facility.

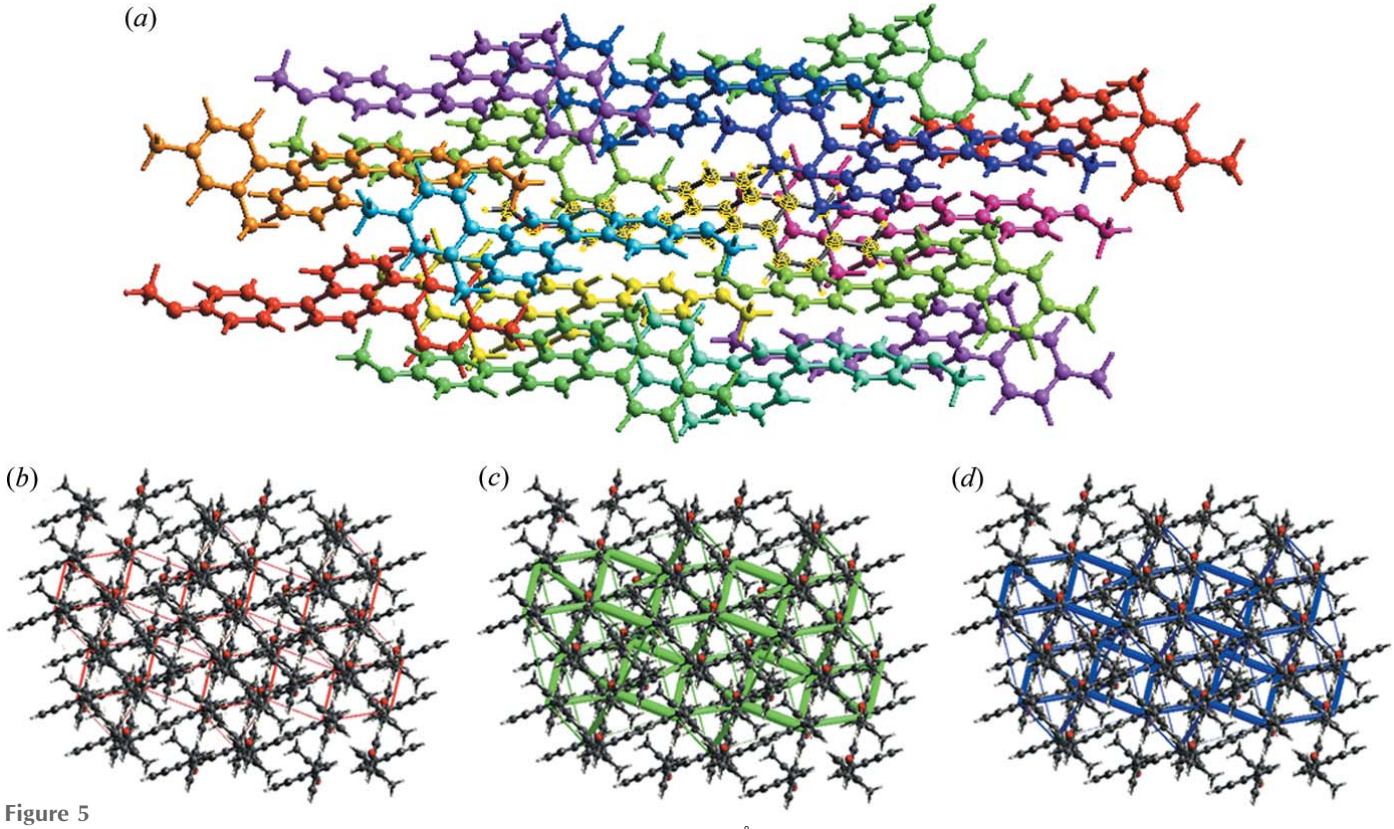

Figure 5
(*a*) Interaction between the selected molecule and the molecules present in a 3.8 Å cluster around it, (*b*) Coulombic energy, (*c*) dispersion energy and (*d*) total energy.

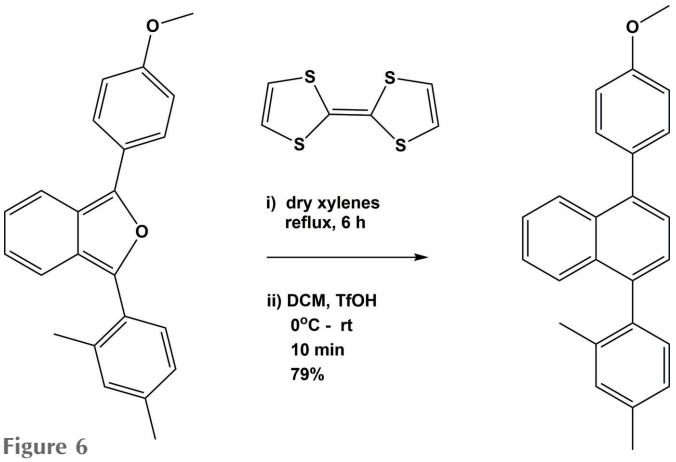

Figure 6
Reaction scheme.

Table 4
Experimental details.

Crystal data	
Chemical formula	$C_{25}H_{22}O$
M_r	338.42
Crystal system, space group	Triclinic, $P\overline{1}$
Temperature (K)	296
a, b, c (Å)	9.1670 (9), 10.4566 (10), 11.2499 (11)
α, β, γ (°)	64.707 (4), 71.312 (4), 77.032 (4)
V (Å^3)	918.75 (16)
Z	2
Radiation type	Mo $K\alpha$
μ (mm^{-1})	0.07
Crystal size (mm)	0.15 × 0.10 × 0.10
Data collection	
Diffractometer	Bruker Kappa APEXII CCD
Absorption correction	Multi-scan (*SADABS*; Bruker, 2012)
T_{min}, T_{max}	0.900, 0.945
No. of measured, independent and observed [$I > 2\sigma(I)$] reflections	19120, 3828, 1777
R_{int}	0.060
(sin $\theta/\lambda)_{max}$ (Å^{-1})	0.631
Refinement	
$R[F^2 > 2\sigma(F^2)]$, $wR(F^2)$, S	0.057, 0.193, 1.00
No. of reflections	3828
No. of parameters	238
H-atom treatment	H-atom parameters constrained
$\Delta\rho_{max}$, $\Delta\rho_{min}$ (e Å^{-3})	0.27, −0.19

Computer programs: *APEX2*, *SAINT* and *XPREP* (Bruker, 2012), *SHELXT2014* (Sheldrick, 2015*a*), *SHELXL2014* (Sheldrick, 2015*b*), *ORTEP-3 for Windows* (Farrugia, 2012) and *Mercury* (Macrae *et al.*, 2008).

References

Bruker (2012). *APEX2*, *SAINT*, *XPREP* and *SADABS*. Bruker AXS Inc., Madison, Wisconsin, USA.

Cai, J., Lin, Y., Yu, J., Wu, C., Chen, L., Cui, Y., Yang, Y., Chen, B. & Qian, G. (2014). *RSC Adv.* **4**, 49457–49461.

Chen, F., Bai, D., Jiang, D., Wang, Y. & He, H. (2017). *Dalton Trans.* **46**, 11469–11478.

Farrugia, L. J. (2012). *J. Appl. Cryst.* **45**, 849–854.

Groom, C. R., Bruno, I. J., Lightfoot, M. P. & Ward, S. C. (2016). *Acta Cryst.* B**72**, 171–179.

Jayatilaka, D., Grimwood, D. J., Lee, A., Lemay, A., Russel, A. J., Taylor, C., Wolff, S. K., Cassam-Chenai, P. & Whitton, A. (2005). *TONTO – A System for Computational Chemistry*. Available at: http://hirshfeldsurface.net/

Lima, C. F. R. A. C., Rocha, M. A. A., Schröder, B., Gomes, L. R., Low, J. N. & Santos, L. M. N. B. F. (2012). *J. Phys. Chem. B*, **116**, 3557–3570.

Lin, X., Telepeni, I., Blake, A. J., Dailly, A., Brown, C. M., Simmons, J. M., Zoppi, M., Walker, G. S., Thomas, K. M., Mays, T. J., Hubberstey, P., Champness, N. R. & Schröder, M. (2009). *J. Am. Chem. Soc.* **131**, 2159–2171.

Mackenzie, C. F., Spackman, P. R., Jayatilaka, D. & Spackman, M. A. (2017). *IUCrJ*, **4**, 575–587.

Macrae, C. F., Bruno, I. J., Chisholm, J. A., Edgington, P. R., McCabe, P., Pidcock, E., Rodriguez-Monge, L., Taylor, R., van de Streek, J. & Wood, P. A. (2008). *J. Appl. Cryst.* **41**, 466–470.

McKinnon, J. J., Jayatilaka, D. & Spackman, M. A. (2007). *Chem. Commun.* pp. 3814–3816.

Rokade, Y. B. & Sayyed, R. Z. (2009). *Rasayan J. Chem.* **2**, 972–980.

Sheldrick, G. M. (2015*a*). *Acta Cryst.* A**71**, 3–8.

Sheldrick, G. M. (2015*b*). *Acta Cryst.* C**71**, 3–8.

Spackman, M. A., McKinnon, J. J. & Jayatilaka, D. (2008). *CrystEngComm*, **10**, 377–388.

Turner, M. J., McKinnon, J. J., Wolff, S. K., Grimwood, D. J., Spackman, P. R., Jayatilaka, D. & Spackman, M. A. (2017). CrystalExplorer 17.5. The University of Western Australia.

Upadhayaya, R. S., Vandavasi, J. K., Kardile, R. A., Lahore, S. V., Dixit, S. S., Deokar, H. S., Shinde, P. D., Sarmah, M. P. & Chattopadhyaya, J. (2010). *Eur. J. Med. Chem.* **45**, 1854–1867.

Wright, M. S., Lax, A. R., Henderson, G. & Chen, J. A. (2000). *Mycologia*, **92**, 42–45.

supporting information

Acta Cryst. (2018). E**74**, 939-943 [https://doi.org/10.1107/S2056989018008332]

Crystal structure and Hirshfeld surface analysis and energy frameworks of 1-(2,4-dimethylphenyl)-4-(4-methoxyphenyl)naphthalene

U. Mohamooda Sumaya, J. KarunaKaran, K. Biruntha, A. K. MohanaKrishnan and G. Usha

Computing details

Data collection: *APEX2* (Bruker, 2012); cell refinement: *APEX2* and *SAINT* (Bruker, 2012); data reduction: *SAINT* and *XPREP* (Bruker, 2012); program(s) used to solve structure: SHELXT2014 (Sheldrick, 2015a); program(s) used to refine structure: *SHELXL2014* (Sheldrick, 2015b); molecular graphics: *ORTEP-3 for Windows* (Farrugia, 2012) and *Mercury* (Macrae *et al.*, 2008); software used to prepare material for publication: *SHELXL2014* (Sheldrick, 2015b).

1-(2,4-Dimethylphenyl)-4-(4-methoxyphenyl)naphthalene

Crystal data

$C_{25}H_{22}O$
M_r = 338.42
Triclinic, $P\overline{1}$
a = 9.1670 (9) Å
b = 10.4566 (10) Å
c = 11.2499 (11) Å
α = 64.707 (4)°
β = 71.312 (4)°
γ = 77.032 (4)°
V = 918.75 (16) Å^3
Z = 2
$F(000)$ = 360
D_x = 1.223 Mg m^{-3}
Mo $K\alpha$ radiation, λ = 0.71073 Å
Cell parameters from 19154 reflections
θ = 2.3–22.7°
μ = 0.07 mm^{-1}
T = 296 K
Block, yellow
0.15 × 0.10 × 0.10 mm

Data collection

Bruker Kappa APEXII CCD diffractometer
Radiation source: fine-focus sealed tube
ω and φ scan
Absorption correction: multi-scan (SADABS; Bruker, 2012)
T_{min} = 0.900, T_{max} = 0.945
19120 measured reflections
3828 independent reflections
1777 reflections with $I > 2\sigma(I)$
R_{int} = 0.060
θ_{max} = 26.6°, θ_{min} = 2.1°
h = −11→11
k = −13→13
l = −14→14

Refinement

Refinement on F^2
Least-squares matrix: full
$R[F^2 > 2\sigma(F^2)]$ = 0.057
$wR(F^2)$ = 0.193
S = 1.00
3828 reflections
238 parameters
0 restraints
Primary atom site location: structure-invariant direct methods
Secondary atom site location: difference Fourier map
Hydrogen site location: inferred from neighbouring sites
H-atom parameters constrained

$w = 1/[\sigma^2(F_o^2) + (0.0922P)^2 + 0.0768P]$
where $P = (F_o^2 + 2F_c^2)/3$
$(\Delta/\sigma)_{max} < 0.001$

$\Delta\rho_{max} = 0.27$ e Å^{-3}
$\Delta\rho_{min} = -0.19$ e Å^{-3}

Special details

Geometry. All esds (except the esd in the dihedral angle between two l.s. planes) are estimated using the full covariance matrix. The cell esds are taken into account individually in the estimation of esds in distances, angles and torsion angles; correlations between esds in cell parameters are only used when they are defined by crystal symmetry. An approximate (isotropic) treatment of cell esds is used for estimating esds involving l.s. planes.

Fractional atomic coordinates and isotropic or equivalent isotropic displacement parameters (Å²)

	x	*y*	*z*	U_{iso}*/U_{eq}
C1	0.7907 (4)	0.8345 (4)	0.2984 (3)	0.0771 (10)
H1A	0.7017	0.8047	0.2937	0.116*
H1B	0.7750	0.9350	0.2771	0.116*
H1C	0.8053	0.7849	0.3885	0.116*
C2	0.9307 (3)	0.8015 (3)	0.1987 (3)	0.0509 (7)
C3	1.0610 (3)	0.8748 (3)	0.1542 (3)	0.0578 (8)
H3	1.0583	0.9411	0.1898	0.069*
C4	1.1927 (3)	0.8530 (3)	0.0602 (3)	0.0573 (8)
C5	1.3309 (4)	0.9324 (4)	0.0196 (4)	0.0863 (11)
H5A	1.4237	0.8679	0.0169	0.129*
H5B	1.3205	0.9724	0.0848	0.129*
H5C	1.3365	1.0071	−0.0686	0.129*
C6	1.1935 (3)	0.7571 (3)	0.0065 (3)	0.0598 (8)
H6	1.2803	0.7415	−0.0585	0.072*
C7	1.0668 (3)	0.6835 (3)	0.0480 (3)	0.0541 (7)
H7	1.0699	0.6198	0.0093	0.065*
C8	0.9353 (3)	0.7015 (3)	0.1453 (3)	0.0446 (7)
C9	0.8049 (3)	0.6158 (3)	0.1869 (3)	0.0437 (6)
C10	0.7284 (3)	0.6328 (3)	0.0942 (3)	0.0537 (7)
H10	0.7534	0.7037	0.0079	0.064*
C11	0.6138 (3)	0.5472 (3)	0.1247 (3)	0.0527 (7)
H11	0.5648	0.5633	0.0581	0.063*
C12	0.5716 (3)	0.4408 (3)	0.2488 (3)	0.0426 (6)
C13	0.6437 (3)	0.4220 (3)	0.3514 (2)	0.0393 (6)
C14	0.7621 (3)	0.5075 (3)	0.3195 (2)	0.0403 (6)
C15	0.8360 (3)	0.4807 (3)	0.4219 (3)	0.0507 (7)
H15	0.9173	0.5323	0.4017	0.061*
C16	0.7907 (3)	0.3810 (3)	0.5493 (3)	0.0602 (8)
H16	0.8414	0.3649	0.6147	0.072*
C17	0.6690 (3)	0.3029 (3)	0.5823 (3)	0.0612 (8)
H17	0.6361	0.2374	0.6706	0.073*
C18	0.5983 (3)	0.3221 (3)	0.4860 (3)	0.0518 (7)
H18	0.5180	0.2682	0.5092	0.062*
C19	0.4540 (3)	0.3483 (3)	0.2743 (2)	0.0432 (6)
C20	0.3108 (3)	0.4064 (3)	0.2491 (3)	0.0504 (7)
H20	0.2877	0.5046	0.2182	0.060*

C21	0.2007 (3)	0.3235 (3)	0.2682 (3)	0.0525 (7)
H21	0.1051	0.3658	0.2507	0.063*
C22	0.2331 (3)	0.1787 (3)	0.3130 (3)	0.0510 (7)
C23	0.3750 (3)	0.1177 (3)	0.3379 (3)	0.0601 (8)
H23	0.3977	0.0195	0.3676	0.072*
C24	0.4841 (3)	0.2011 (3)	0.3193 (3)	0.0543 (7)
H24	0.5794	0.1581	0.3371	0.065*
C25	−0.0236 (4)	0.1430 (4)	0.3343 (4)	0.0834 (11)
H25A	−0.0854	0.0667	0.3644	0.125*
H25B	−0.0284	0.2070	0.2437	0.125*
H25C	−0.0624	0.1932	0.3942	0.125*
O1	0.1324 (2)	0.0867 (2)	0.3352 (2)	0.0742 (7)

Atomic displacement parameters (Å²)

	U^{11}	U^{22}	U^{33}	U^{12}	U^{13}	U^{23}
C1	0.076 (2)	0.079 (2)	0.081 (2)	−0.0173 (19)	−0.0011 (18)	−0.044 (2)
C2	0.0503 (17)	0.0521 (17)	0.0505 (17)	−0.0106 (14)	−0.0132 (14)	−0.0171 (14)
C3	0.068 (2)	0.0485 (17)	0.0622 (19)	−0.0158 (15)	−0.0235 (16)	−0.0169 (15)
C4	0.0534 (18)	0.0526 (18)	0.0532 (18)	−0.0149 (15)	−0.0173 (15)	−0.0013 (15)
C5	0.069 (2)	0.091 (3)	0.088 (3)	−0.040 (2)	−0.0228 (19)	−0.007 (2)
C6	0.0523 (18)	0.0585 (19)	0.0533 (18)	−0.0127 (15)	−0.0040 (14)	−0.0106 (16)
C7	0.0547 (17)	0.0528 (18)	0.0498 (17)	−0.0128 (14)	−0.0061 (14)	−0.0169 (14)
C8	0.0491 (16)	0.0419 (15)	0.0427 (15)	−0.0124 (13)	−0.0133 (13)	−0.0113 (13)
C9	0.0458 (15)	0.0475 (16)	0.0415 (15)	−0.0104 (13)	−0.0101 (12)	−0.0186 (13)
C10	0.0621 (18)	0.0550 (18)	0.0421 (16)	−0.0192 (15)	−0.0150 (14)	−0.0093 (14)
C11	0.0593 (18)	0.0571 (18)	0.0424 (17)	−0.0159 (15)	−0.0180 (14)	−0.0113 (14)
C12	0.0412 (15)	0.0454 (15)	0.0438 (16)	−0.0070 (12)	−0.0088 (12)	−0.0197 (13)
C13	0.0393 (14)	0.0416 (15)	0.0365 (15)	−0.0044 (12)	−0.0067 (11)	−0.0165 (12)
C14	0.0404 (14)	0.0416 (15)	0.0408 (15)	−0.0055 (12)	−0.0091 (12)	−0.0178 (13)
C15	0.0515 (16)	0.0574 (18)	0.0482 (17)	−0.0131 (14)	−0.0149 (14)	−0.0197 (15)
C16	0.069 (2)	0.070 (2)	0.0467 (18)	−0.0158 (17)	−0.0230 (15)	−0.0174 (16)
C17	0.073 (2)	0.067 (2)	0.0392 (17)	−0.0215 (17)	−0.0110 (15)	−0.0115 (15)
C18	0.0526 (17)	0.0563 (18)	0.0454 (17)	−0.0149 (14)	−0.0063 (13)	−0.0185 (15)
C19	0.0435 (15)	0.0456 (16)	0.0436 (15)	−0.0065 (13)	−0.0088 (12)	−0.0206 (13)
C20	0.0522 (17)	0.0465 (16)	0.0551 (17)	−0.0068 (14)	−0.0183 (13)	−0.0179 (14)
C21	0.0458 (16)	0.0576 (19)	0.0610 (18)	−0.0057 (14)	−0.0174 (13)	−0.0261 (15)
C22	0.0521 (18)	0.0548 (19)	0.0544 (18)	−0.0148 (15)	−0.0075 (14)	−0.0285 (15)
C23	0.060 (2)	0.0463 (17)	0.076 (2)	−0.0056 (16)	−0.0136 (16)	−0.0280 (16)
C24	0.0451 (16)	0.0518 (18)	0.0666 (19)	−0.0019 (14)	−0.0130 (14)	−0.0256 (15)
C25	0.060 (2)	0.102 (3)	0.108 (3)	−0.029 (2)	−0.0172 (19)	−0.051 (2)
O1	0.0641 (14)	0.0687 (14)	0.1023 (18)	−0.0233 (12)	−0.0140 (12)	−0.0415 (13)

Geometric parameters (Å, º)

C1—C2	1.495 (4)	C13—C18	1.413 (3)
C1—H1A	0.9600	C13—C14	1.421 (3)
C1—H1B	0.9600	C14—C15	1.416 (3)

C1—H1C	0.9600	C15—C16	1.360 (4)
C2—C8	1.399 (4)	C15—H15	0.9300
C2—C3	1.401 (3)	C16—C17	1.390 (3)
C3—C4	1.375 (4)	C16—H16	0.9300
C3—H3	0.9300	C17—C18	1.357 (4)
C4—C6	1.373 (4)	C17—H17	0.9300
C4—C5	1.510 (4)	C18—H18	0.9300
C5—H5A	0.9600	C19—C20	1.380 (4)
C5—H5B	0.9600	C19—C24	1.391 (4)
C5—H5C	0.9600	C20—C21	1.383 (3)
C6—C7	1.381 (3)	C20—H20	0.9300
C6—H6	0.9300	C21—C22	1.370 (4)
C7—C8	1.385 (3)	C21—H21	0.9300
C7—H7	0.9300	C22—O1	1.373 (3)
C8—C9	1.488 (3)	C22—C23	1.373 (4)
C9—C10	1.366 (3)	C23—C24	1.381 (3)
C9—C14	1.430 (3)	C23—H23	0.9300
C10—C11	1.397 (3)	C24—H24	0.9300
C10—H10	0.9300	C25—O1	1.420 (4)
C11—C12	1.363 (4)	C25—H25A	0.9600
C11—H11	0.9300	C25—H25B	0.9600
C12—C13	1.430 (3)	C25—H25C	0.9600
C12—C19	1.488 (3)		

C2—C1—H1A	109.5	C18—C13—C12	121.9 (2)
C2—C1—H1B	109.5	C14—C13—C12	119.8 (2)
H1A—C1—H1B	109.5	C15—C14—C13	118.0 (2)
C2—C1—H1C	109.5	C15—C14—C9	121.8 (2)
H1A—C1—H1C	109.5	C13—C14—C9	120.2 (2)
H1B—C1—H1C	109.5	C16—C15—C14	121.4 (3)
C8—C2—C3	118.4 (2)	C16—C15—H15	119.3
C8—C2—C1	122.1 (2)	C14—C15—H15	119.3
C3—C2—C1	119.5 (3)	C15—C16—C17	120.4 (3)
C4—C3—C2	122.9 (3)	C15—C16—H16	119.8
C4—C3—H3	118.5	C17—C16—H16	119.8
C2—C3—H3	118.5	C18—C17—C16	120.1 (3)
C6—C4—C3	117.8 (3)	C18—C17—H17	120.0
C6—C4—C5	121.9 (3)	C16—C17—H17	120.0
C3—C4—C5	120.3 (3)	C17—C18—C13	121.6 (3)
C4—C5—H5A	109.5	C17—C18—H18	119.2
C4—C5—H5B	109.5	C13—C18—H18	119.2
H5A—C5—H5B	109.5	C20—C19—C24	117.0 (2)
C4—C5—H5C	109.5	C20—C19—C12	120.9 (2)
H5A—C5—H5C	109.5	C24—C19—C12	122.1 (2)
H5B—C5—H5C	109.5	C19—C20—C21	122.2 (3)
C4—C6—C7	120.7 (3)	C19—C20—H20	118.9
C4—C6—H6	119.7	C21—C20—H20	118.9
C7—C6—H6	119.7	C22—C21—C20	119.7 (3)

C6—C7—C8	122.1 (3)	C22—C21—H21	120.2
C6—C7—H7	119.0	C20—C21—H21	120.2
C8—C7—H7	119.0	C21—C22—O1	124.4 (3)
C7—C8—C2	118.1 (2)	C21—C22—C23	119.5 (3)
C7—C8—C9	118.8 (2)	O1—C22—C23	116.0 (3)
C2—C8—C9	123.1 (2)	C22—C23—C24	120.5 (3)
C10—C9—C14	117.6 (2)	C22—C23—H23	119.8
C10—C9—C8	120.0 (2)	C24—C23—H23	119.8
C14—C9—C8	122.3 (2)	C23—C24—C19	121.2 (3)
C9—C10—C11	122.3 (3)	C23—C24—H24	119.4
C9—C10—H10	118.9	C19—C24—H24	119.4
C11—C10—H10	118.9	O1—C25—H25A	109.5
C12—C11—C10	122.1 (3)	O1—C25—H25B	109.5
C12—C11—H11	119.0	H25A—C25—H25B	109.5
C10—C11—H11	119.0	O1—C25—H25C	109.5
C11—C12—C13	118.0 (2)	H25A—C25—H25C	109.5
C11—C12—C19	120.0 (2)	H25B—C25—H25C	109.5
C13—C12—C19	122.0 (2)	C22—O1—C25	117.3 (2)
C18—C13—C14	118.4 (2)		

C8—C2—C3—C4	0.2 (4)	C12—C13—C14—C9	2.4 (3)
C1—C2—C3—C4	−178.4 (3)	C10—C9—C14—C15	179.2 (2)
C2—C3—C4—C6	1.4 (4)	C8—C9—C14—C15	3.5 (4)
C2—C3—C4—C5	−178.2 (3)	C10—C9—C14—C13	0.0 (3)
C3—C4—C6—C7	−1.2 (4)	C8—C9—C14—C13	−175.7 (2)
C5—C4—C6—C7	178.4 (3)	C13—C14—C15—C16	−3.2 (4)
C4—C6—C7—C8	−0.7 (4)	C9—C14—C15—C16	177.6 (2)
C6—C7—C8—C2	2.3 (4)	C14—C15—C16—C17	−0.3 (4)
C6—C7—C8—C9	−178.6 (2)	C15—C16—C17—C18	2.4 (4)
C3—C2—C8—C7	−2.0 (4)	C16—C17—C18—C13	−0.9 (4)
C1—C2—C8—C7	176.6 (3)	C14—C13—C18—C17	−2.6 (4)
C3—C2—C8—C9	178.9 (2)	C12—C13—C18—C17	178.8 (3)
C1—C2—C8—C9	−2.5 (4)	C11—C12—C19—C20	−53.8 (3)
C7—C8—C9—C10	−63.5 (3)	C13—C12—C19—C20	126.4 (3)
C2—C8—C9—C10	115.5 (3)	C11—C12—C19—C24	123.9 (3)
C7—C8—C9—C14	112.1 (3)	C13—C12—C19—C24	−56.0 (3)
C2—C8—C9—C14	−68.9 (3)	C24—C19—C20—C21	0.5 (4)
C14—C9—C10—C11	−1.1 (4)	C12—C19—C20—C21	178.2 (2)
C8—C9—C10—C11	174.7 (2)	C19—C20—C21—C22	−0.3 (4)
C9—C10—C11—C12	−0.3 (4)	C20—C21—C22—O1	−179.9 (2)
C10—C11—C12—C13	2.7 (4)	C20—C21—C22—C23	−0.2 (4)
C10—C11—C12—C19	−177.2 (2)	C21—C22—C23—C24	0.6 (4)
C11—C12—C13—C18	174.9 (2)	O1—C22—C23—C24	−179.7 (2)
C19—C12—C13—C18	−5.2 (3)	C22—C23—C24—C19	−0.4 (4)
C11—C12—C13—C14	−3.7 (3)	C20—C19—C24—C23	−0.1 (4)
C19—C12—C13—C14	176.2 (2)	C12—C19—C24—C23	−177.8 (2)
C18—C13—C14—C15	4.5 (3)	C21—C22—O1—C25	−11.4 (4)
C12—C13—C14—C15	−176.8 (2)	C23—C22—O1—C25	168.9 (3)

C18—C13—C14—C9	−176.2 (2)

Hydrogen-bond geometry (Å, º)

Cg is the centroid of the C13–C18 ring.

D—H···*A*	*D*—H	H···*A*	*D*···*A*	*D*—H···*A*
C25—H25*C*···*Cg*^{i}	0.96	2.78	3.597 (5)	144

Symmetry code: (i) *x*−1, *y*, *z*.